

Lower limit of percolation threshold on a square lattice with complex neighborhoods

Antoni Ciephucha,^{*} Marcin Utnicki, Maciej Wołoszyn,[†] and Krzysztof Malarz[‡]

AGH University, Faculty of Physics and Applied Computer Science, al. Mickiewicza 30, 30-059 Kraków, Poland

(Dated: March 24, 2025)

In this paper, the 60-year-old concept of long-range interaction in percolation problems introduced by Dalton, Domb, and Sykes, is reconsidered. With Monte Carlo simulation—based on Newman–Ziff algorithm and finite-size scaling hypothesis—we estimate 64 percolation thresholds for random site percolation problem on a square lattice with neighborhoods that contain sites from the 7th coordination zone. The percolation thresholds obtained range from 0.27013 (for the neighborhood that contains only sites from the 7th coordination zone) to 0.11535 (for the neighborhood that contains all sites from the 1st to the 7th coordination zone). Similarly to neighborhoods with smaller ranges, the power-law dependence of the percolation threshold on the effective coordination number with exponent close to $-1/2$ is observed. Finally, we empirically determine the limit of the percolation threshold on square lattices with complex neighborhoods. This limit scales with the inverse square of the mean radius of the neighborhood. The boundary of this limit is touched for threshold values associated with extended (compact) neighborhoods.

I. INTRODUCTION

The percolation [1–4] (see References [5, 6] for recent reviews) is one of the core topics in statistical physics providing the possibility to look at the critical phenomena occurring at phase transition solely on the geometrical basis, without samples heating, cooling, inserting in a magnetic field, etc. Some problems with respect to percolation can be treated analytically [7–12], but most studies are computational.

Originating from works by Broadbent and Hammersley [13, 14] devoted to rheology (and still applied there [15–18]), it quickly found plenty of applications in physics, including magnetic [19–23] and electric [24–26] properties of solids or nano-engineering [27].

However, the application of percolation theory is not restricted to physics alone. Such examples (mainly two-dimensional systems [28–32]) can also be found in epidemiology [33–35], forest fires [36–40], agriculture [41–43], urbanization [44, 45], materials chemistry [46], sociology [47], psychology [48], information transfer [49], finances [50], or dentistry [51].

On the other hand, some effort was put into studying percolation on cubic ($d = 3$ [52–57]) and hyper-cubic lattices, also for non-physical dimensions ($d = 4$ [52, 58–60], $d = 5$ [52, 60, 61] and higher $d \geq 6$ [52, 62, 63]). Simultaneously, the complex [6, 49, 64], distorted [65–67] and fractal [68] networks were studied.

Recently, the 60-year-old concept of long-range interaction [69, 70] has sparked renewed interest. The neighborhood that contains sites that are not nearest-neighbors on assumed lattice are called extended neighborhoods (when they are compact) or complex (when they are non-compact, that is, they contain ‘wholes’)—to keep the

nomenclature from Reference [71]. Many papers were devoted to studies of the percolation thresholds on the extended [49, 59, 61, 72–74] and the complex [57, 58, 71, 75–82] neighborhoods.

The particular neighborhoods names—now keeping the convention proposed in Reference [83]—are combination of alphanumeric strings. The first two letters identify the underlying lattice (for example: SQ for square, TR for triangular, HC for honeycomb, and SC for simple cubic lattices) then they are accompanied with numerical string indicating coordination zones which constitute the neighborhood. In this convention, the von Neumann neighborhood on the square lattice (with only the nearest neighbors) is called SQ-1, while Moore’s neighborhood on square lattice (containing sites from the first and the second coordination zones) is called SQ-1,2.

In this paper we are closer to the theoretical studies of percolation phenomena than to its application. That is, our studies focus on the influence of long-range interactions on the percolation threshold p_c . The percolation threshold is the equivalent of the critical point in the phase-transition phenomena. For the random site percolation problem, we deal with the nodes of the lattice that are occupied (with probability p) or empty (with probability $1 - p$). Occupied sites, in assumed neighborhood, are considered to form a cluster. Depending on the sites occupation probability p such cluster may span (or not) the system edges. The percolation threshold p_c is such an occupation probability p , that for $p < p_c$ a spanning cluster is absent (and the system behaves as an insulator), while for $p > p_c$ a spanning cluster is present (and the system behaves as a conductor). Thus, p_c separates two phases: isolating and conducting, and at $p = p_c$ the (second-order) phase transition takes place.

Here, we calculate the percolation thresholds p_c for random site percolation in the square lattice for neighborhoods containing sites from the 7th coordination zone. There are 64 such neighborhoods, from SQ-7 to SQ-1,2,3,4,5,6,7, and they are presented in Figure 1.

The paper is organized as follows: in Section II we re-

^{*} 0009-0006-4018-7027

[†] 0000-0001-9896-1018

[‡] 0000-0001-9980-0363; malarz@agh.edu.pl

call the finite-size scaling hypothesis, present basics of the effective Newman–Ziff Monte Carlo algorithm for the percolation problem, define the effective coordination number and give some details regarding technicalities of computations. In Section III we show the results of Monte Carlo simulations which allow for the estimation of 64 values of p_c for various neighborhoods together with their geometrical characteristics, such as total and effective coordination numbers. Finally, Section IV is devoted to a discussion of the obtained results.

II. METHODS

A. Finite-Size Scaling Hypothesis

In the vicinity of the critical point x_c , many observables X obey the finite-size scaling [1, 84, 85] relation

$$X(x; L) = L^{-\varepsilon_1} \cdot \mathcal{F}((x - x_c)L^{\varepsilon_2}), \quad (1)$$

where x reflects the level of system disorder, \mathcal{F} is the scaling function (usually analytically unknown), and $\varepsilon_{1,2}$ are universal exponents. These exponents depend only on the physical dimension of the system d . Knowing $\varepsilon_{1,2}$ and plotting $X(x; L)$ leads to the collapse of many curves (for various L) into a single one.

At the critical point $x = x_c$, the value of

$$X(x = x_c; L) \cdot L^{\varepsilon_1} = \mathcal{F}(0) \quad (2)$$

does not depend on the size of the system L , which opens a computationally feasible way of searching for both the critical point x_c and the critical exponents $\varepsilon_{1,2}$.

For the random site percolation problem, the probability

$$P_{\max} = S_{\max}/L^2, \quad (3)$$

that the randomly chosen site belongs to the largest cluster (with size S_{\max}), may play the role of the quantity X . Then, the exponents $\varepsilon_{1,2}$ are known analytically, and $\varepsilon_1 = 5/48$ while $\varepsilon_2 = 3/4$.

B. Efficient Newman–Ziff Algorithm

To calculate the probability P_{\max} mentioned above we use Newman and Ziff algorithm [86]. The algorithm is fast as it is based on the concept of calculating desired quantities only after adding a single occupied site to the so far existing system. This allows us to construct the dependence of $X(n)$, where n is the number of occupied sites.

The second part of the algorithm is the transformation of $X(n)$ values from the space of the integer number n of occupied sites to $X(p)$ in the space of the real numbers of probabilities p of sites occupation

$$X(p; N) = \sum_{n=0}^N \bar{X}(n; N) \mathcal{B}(n; N, p), \quad (4)$$

where $N = L^2$ stands for the size of the system. This conversion requires knowing the Bernoulli (binomial) probability distribution

$$\mathcal{B}(n; N, p) = \binom{N}{n} p^n (1-p)^{N-n} \quad (5)$$

and Reference [86] provides an efficient way of recursive calculation of the binomial distribution coefficients in Equation (5).

We implement the Newman and Ziff algorithm as a computer program written in C language. This requires modification of the original `boundaries()` procedure provided in Reference [86] beyond the nearest neighbors. In Listing 1, available in Appendix A, we show an example of such modification for the sq-7 neighborhood presented in Figure 1.1.

C. Effective Coordination Number

The values of p_c usually degenerate strongly with respect to the neighborhood coordination number z . Degeneration means that for a given coordination number (number of sites in the neighborhood), many various values of p_c are associated with this coordination number z . This degeneration may be removed (at least partially) when instead of dealing with the coordination number z , we use the effective coordination number

$$\zeta = \sum_i z_i r_i, \quad (6)$$

where z_i and r_i are the number of sites and their distance from the central site in the neighborhood in the i -th coordination zone [81, 82], respectively. Very recently, it was shown that for square, honeycomb and triangular lattices

$$p_c(\zeta) \propto \zeta^{-w} \quad (7)$$

and exponent $w \approx 1/2$ [71].

III. RESULTS

In Figure 2 we present the dependencies of the probabilities P_{\max} of belonging to the largest cluster on sites occupation probability n/L^2 . P_{\max} values are defined by geometrical probability as the size of the largest cluster S_{\max} per the system size L^2 . The results are averaged over $R = 10^5$ realizations of systems that contain 128^2 , 256^2 , 512^2 , 1024^2 , 2048^2 and 4096^2 sites. The examples correspond to the neighborhoods sq-7 (Figure 2.1) and sq-1,2,3,4,5,6,7 (Figure 2.2).

In Figure 3 examples of dependencies of $P_{\max} L^{\beta/\nu}$ versus p are presented for various linear system sizes L . The examples correspond to the neighborhoods sq-1 (Figure 3.1) and sq-1,2,3,4,5,6,7 (Figure 3.2). These dependencies for 64 neighborhoods containing sites from the

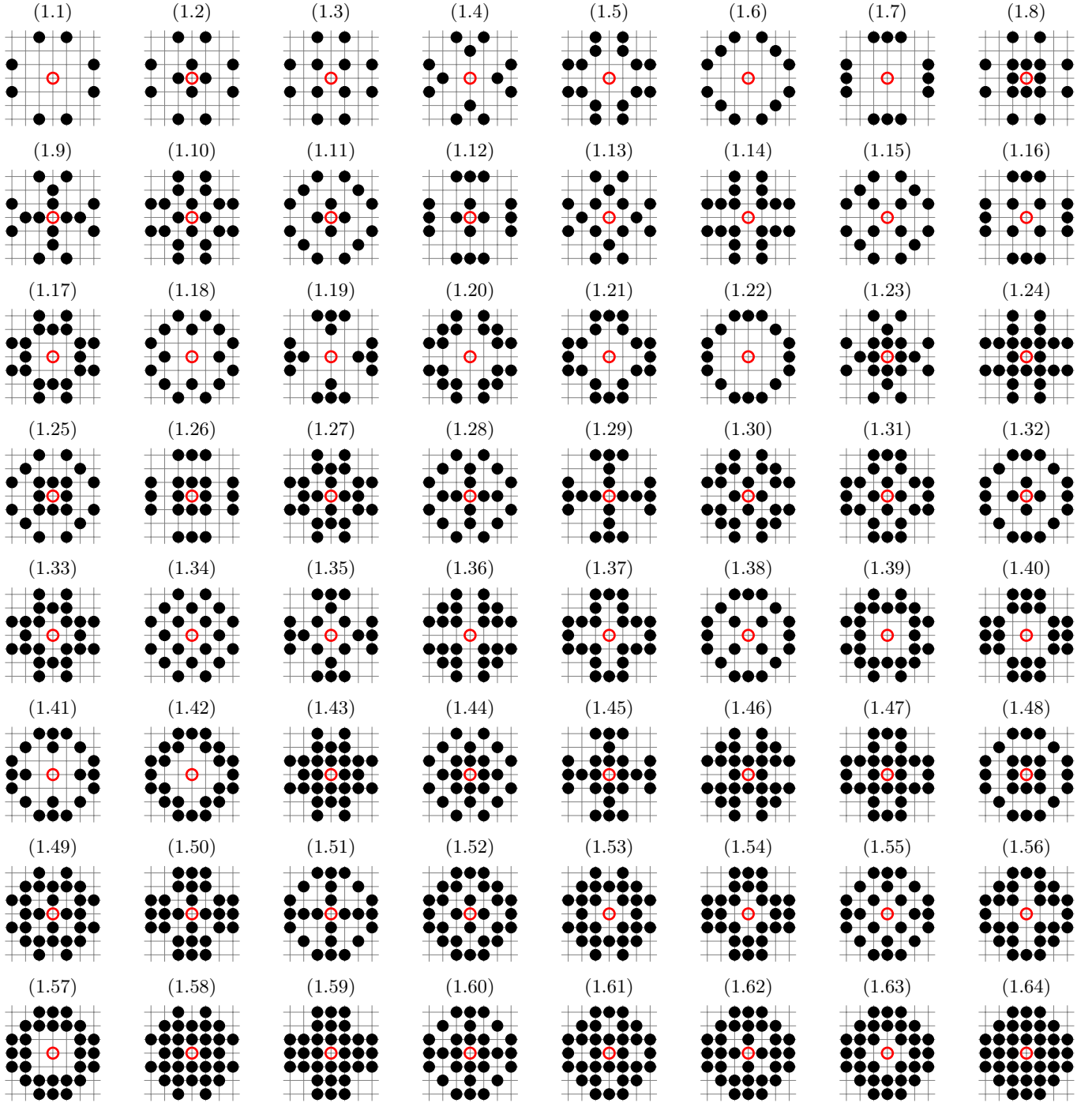


FIG. 1: Neighborhoods on square lattice containing sites from the 7-th coordination zone: (1.1) SQ-7, (1.2) SQ-1,7, (1.3) SQ-2,7, (1.4) SQ-3,7, (1.5) SQ-4,7, (1.6) SQ-5,7, (1.7) SQ-6,7, (1.8) SQ-1,2,7, (1.11) SQ-1,5,7, (1.12) SQ-1,6,7, (1.13) SQ-2,3,7, (1.14) SQ-2,4,7, (1.15) SQ-2,5,7, (1.16) SQ-2,6,7, (1.17) SQ-3,4,7, (1.18) SQ-3,5,7, (1.19) SQ-3,6,7, (1.20) SQ-4,5,7, (1.21) SQ-4,6,7, (1.22) SQ-5,6,7, (1.23) SQ-1,2,3,7, (1.24) SQ-1,2,4,7, (1.25) SQ-1,2,5,7, (1.26) SQ-1,2,6,7, (1.27) SQ-1,3,4,7, (1.28) SQ-1,3,5,7, (1.29) SQ-1,3,6,7, (1.30) SQ-1,4,5,7, (1.31) SQ-1,4,6,7, (1.32) SQ-1,5,6,7, (1.33) SQ-2,3,4,7, (1.34) SQ-2,3,5,7, (1.35) SQ-2,3,6,7, (1.36) SQ-2,4,5,7, (1.37) SQ-2,4,6,7, (1.38) SQ-2,5,6,7, (1.39) SQ-3,4,5,7, (1.40) SQ-3,4,6,7, (1.41) SQ-3,5,6,7, (1.42) SQ-4,5,6,7, (1.43) SQ-1,2,3,4,7, (1.44) SQ-1,2,3,5,7, (1.45) SQ-1,2,3,6,7, (1.46) SQ-1,2,4,5,7, (1.47) SQ-1,2,4,6,7, (1.48) SQ-1,2,5,6,7, (1.49) SQ-1,3,4,5,7, (1.50) SQ-1,3,4,6,7, (1.51) SQ-1,3,5,6,7, (1.52) SQ-1,4,5,6,7, (1.53) SQ-2,3,4,5,7, (1.54) SQ-2,3,4,6,7, (1.55) SQ-2,3,5,6,7, (1.56) SQ-2,4,5,6,7, (1.57) SQ-3,4,5,6,7, (1.58) SQ-1,2,3,4,5,7, (1.59) SQ-1,2,3,4,6,7, (1.60) SQ-1,2,3,5,6,7, (1.61) SQ-1,2,4,5,6,7, (1.62) SQ-1,3,4,5,6,7, (1.63) SQ-2,3,4,5,6,7, (1.64) SQ-1,2,3,4,5,6,7

7th coordination zone are presented in Figure 1 in the Supplemental Material [87]. The common cross-point for various lattice sizes predicts the percolation threshold p_c .

The evaluated percolation thresholds p_c , the total (z) and the effective (ζ) coordination numbers for various neighborhoods are collected in Table I.

In Figure 4 the dependencies of the percolation threshold p_c on the total (z , Figure 4.1) and effective (ζ , Figure 4.2) are presented. Figure 4.3 shows $p_c(\zeta)$ with additional data also for neighborhoods containing sites up to the 6th coordination zone [71]. The inflated neighborhoods (marked by \times) are excluded from the fitting procedure. The data are accompanied by the least squares method fit to the power law (7). The estimated value of the exponent $w \approx 0.5552(42)$.

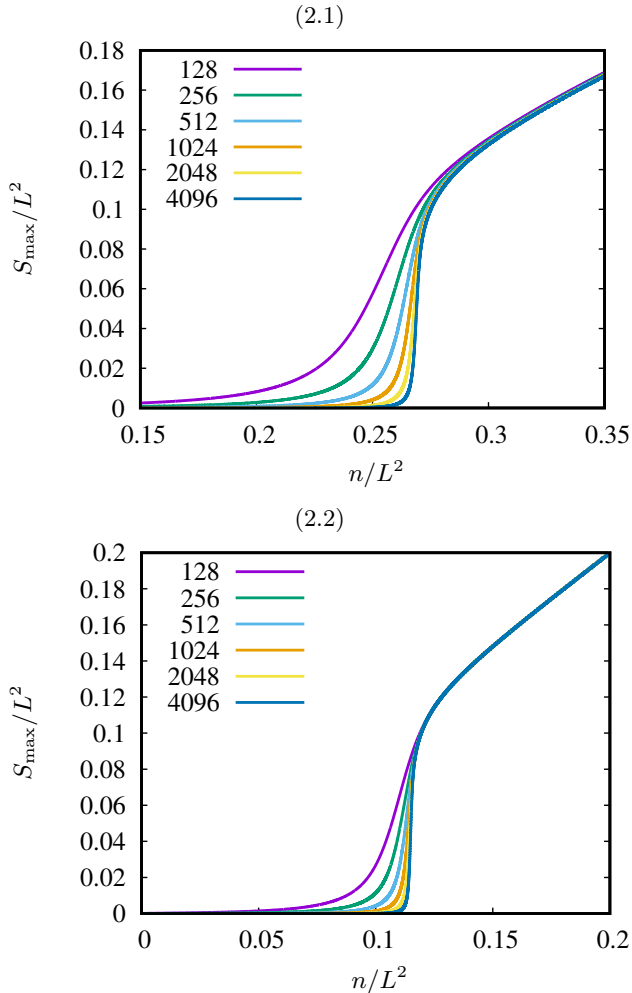


FIG. 2: Examples of dependencies of S_{\max}/L^2 versus n/L^2 for various linear system sizes $L = 128, 256, 512, 1024, 2048$ and 4096 from top to bottom. (2.1) SQ-7, (2.2) SQ-1,2,3,4,5,6,7

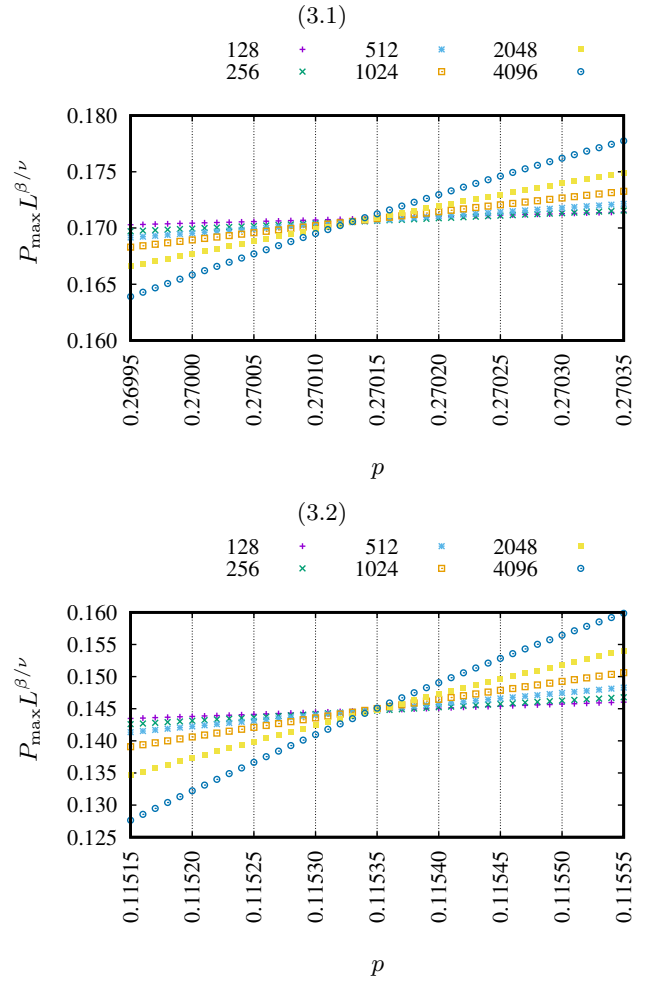


FIG. 3: Examples of dependencies of $P_{\max}L^{\beta/\nu}$ versus p for various linear system sizes $L = 128, 256, 512, 1024, 2048$ and 4096 from top to bottom. (3.1) SQ-7, $p_c(\text{SQ-7}) = 0.27013$, (3.2) SQ-1,2,3,4,5,6,7, $p_c(\text{SQ-1,2,3,4,5,6,7}) = 0.11535$

IV. DISCUSSION

In this paper, the estimation of p_c for random site percolation on the square lattice for neighborhoods containing sites from the 7th coordination zone is presented. Monte Carlo simulation with $R = 10^5$ system realizations for the system sizes from 128^2 to 4096^2 sites allowed us to estimate the percolation thresholds to the 10^{-5} accuracy.

The obtained percolation thresholds range from 0.27013 (for the neighborhood that contains solely sites from the 7th coordination zone) to 0.11535 (for the neighborhood that contains all sites from the 1st to the 7th coordination zone). The latter agrees perfectly (with the accuracy obtained here, that is 10^{-5}) with the earlier results of the extensive Monte Carlo simulation (with $L = 16384$ and $R > 3 \cdot 10^8$ independent samples produced for each lattice) where $p_c(\text{SQ-1,2,3,4,5,6,7}) \approx 0.1153481(9)$ [72].

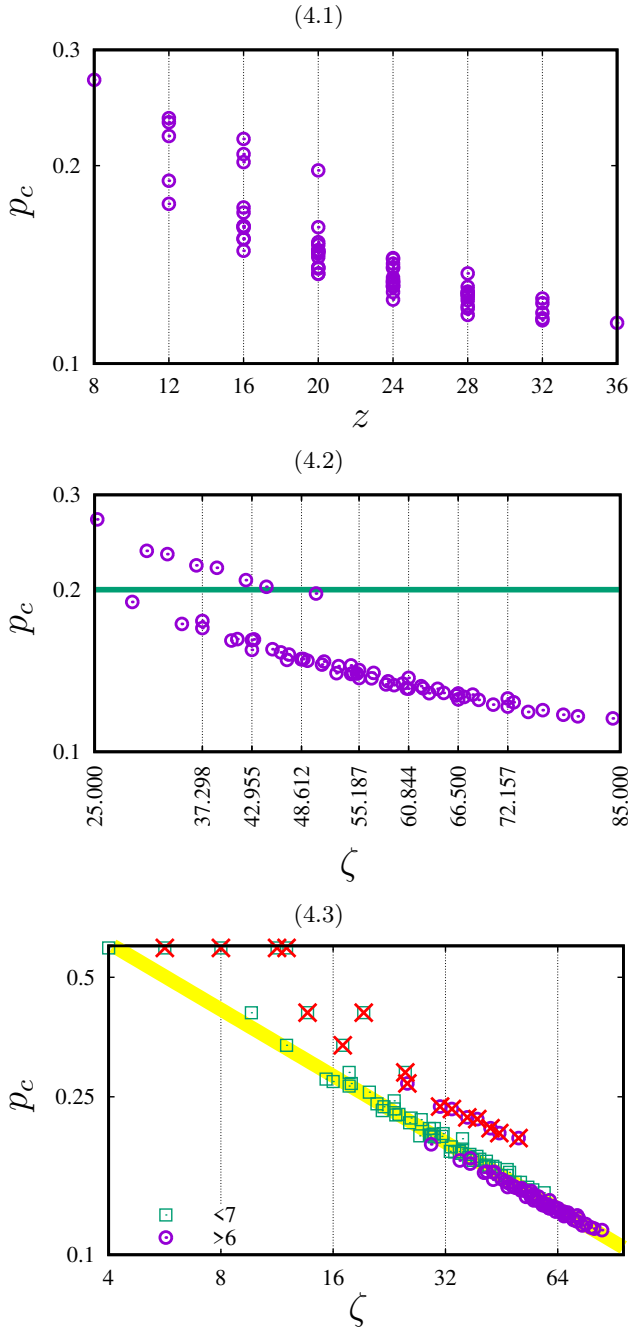


FIG. 4: Dependencies of p_c on (4.1) the total (z) and (4.2) effective (ζ) coordination number for neighborhoods presented in Figure 1. (4.3) $p_c(\zeta)$ with additional data also for neighborhoods (marked by \square) containing sites up to the 6th coordination zone (after Reference [71] and references therein). The inflated neighborhoods (marked by \times) are excluded from the fitting procedure. The least-squares fit gives exponent $w \approx 0.5552(42)$

TABLE I: Percolation thresholds p_c for a square lattice with complex neighborhoods (and their characteristics z, ζ) containing sites from the 7th coordination zone presented in Figure 1

lattice	z	ζ	p_c
sq-1,2,3,4,5,6,7	36	84.157	0.11535
sq-2,3,4,5,6,7	32	80.157	0.11636
sq-1,3,4,5,6,7	32	78.500	0.11719
sq-1,2,4,5,6,7	32	76.157	0.11949
sq-1,2,3,5,6,7	28	66.269	0.12725
sq-1,2,3,4,6,7	32	72.844	0.12358
sq-1,2,3,4,5,7	32	72.157	0.12562
sq-3,4,5,6,7	28	74.500	0.11859
sq-2,4,5,6,7	28	72.157	0.12132
sq-2,3,5,6,7	24	62.269	0.13241
sq-2,3,4,6,7	28	68.844	0.12488
sq-2,3,4,5,7	28	68.157	0.12770
sq-1,4,5,6,7	28	70.500	0.12236
sq-1,3,5,6,7	24	60.612	0.13112
sq-1,3,4,6,7	28	67.187	0.12644
sq-1,3,4,5,7	28	66.500	0.12830
sq-1,2,5,6,7	24	58.269	0.13339
sq-1,2,4,6,7	28	64.844	0.12864
sq-1,2,4,5,7	28	64.157	0.13089
sq-1,2,3,6,7	24	54.955	0.13973
sq-1,2,3,5,7	24	54.269	0.14470
sq-1,2,3,4,7	28	60.844	0.13718
sq-4,5,6,7	24	66.500	0.12513
sq-3,5,6,7	20	56.612	0.13689
sq-3,4,6,7	24	63.187	0.12848
sq-3,4,5,7	24	62.500	0.13121
sq-2,5,6,7	20	54.269	0.13959
sq-2,4,6,7	24	60.844	0.13104
sq-2,4,5,7	24	60.157	0.13386
sq-2,3,6,7	20	50.955	0.14523
sq-2,3,5,7	20	50.269	0.19672
sq-2,3,4,7	24	56.844	0.14015
sq-1,5,6,7	20	52.612	0.13998
sq-1,4,6,7	24	59.187	0.13298
sq-1,4,5,7	24	58.500	0.13515
sq-1,3,6,7	20	49.298	0.14760
sq-1,3,5,7	20	48.612	0.14876
sq-1,3,4,7	24	55.187	0.14187
sq-1,2,6,7	20	46.955	0.14814
sq-1,2,5,7	20	46.269	0.15298
sq-1,2,4,7	24	52.844	0.14423
sq-1,2,3,7	20	42.955	0.16125
sq-5,6,7	16	48.612	0.14848
sq-4,6,7	20	55.187	0.13708
sq-4,5,7	20	54.500	0.14008
sq-3,6,7	16	45.298	0.15503
sq-3,5,7	16	44.612	0.20250
sq-3,4,7	20	51.187	0.14709
sq-2,6,7	16	42.955	0.15461
sq-2,5,7	16	42.269	0.20831
sq-2,4,7	20	48.844	0.14868
sq-2,3,7	16	38.955	0.21963
sq-1,6,7	16	41.298	0.16193
sq-1,5,7	16	40.612	0.16095
sq-1,4,7	20	47.187	0.15157
sq-1,3,7	16	37.298	0.16973
sq-1,2,7	16	34.955	0.17278
sq-6,7	12	37.298	0.17497
sq-5,7	12	36.612	0.22190
sq-4,7	16	43.187	0.16171
sq-3,7	12	33.298	0.23288
sq-2,7	12	30.955	0.23619
sq-1,7	12	29.298	0.18976
sq-7	8	25.298	0.27013

Capturing the intersection of the rescaled probabilities of belonging to the largest cluster $L^{\beta/\nu} \cdot P_{\max}(p)$ numerically for finite systems is quite challenging as the curves for various L rather seldom intersect exactly at one point

(as predicted theoretically by Equation (2)). Also in our case, in Figure 3, we do not have the intersection of the $L^{\beta/\nu} \cdot P_{\max}(p)$ curves for different L occurring at one point, but rather we can easily identify the value of p^* for which the mutual squared differences

$$\delta^2(p) = \sum_{i,j} \left[L_i^{\beta/\nu} \cdot P_{\max}(p; L_i) - L_j^{\beta/\nu} \cdot P_{\max}(p; L_j) \right]^2$$

between the $L^{\beta/\nu} \cdot P_{\max}(p)$ values—for all studied L —is the smallest. This value of p^* for which the mutual squared differences $\delta^2(p)$ reaches its minimum estimates the percolation threshold $p_c \approx p^*$ [88]. The convolution (4) can be performed for any arbitrary value of p , but the secret of achieving such a small δ^2 value that one has the impression it tends to zero lies in the reasonable assumption of the separation Δp with which we scan p values. In Figure 5 we show examples of $L^{\beta/\nu} \cdot P_{\max}(p)$ for $\Delta p = 10^{-4}$, 10^{-5} and 10^{-6} . As can be seen, these dependencies allow us to easily indicate the “intersection point” for $\Delta p = 10^{-4}$ (Figure 5.1) and 10^{-5} (Figure 5.2). That is, just by inspection, even without calculating δ^2 , one can see a higher dispersion of the values $L^{\beta/\nu} \cdot P_{\max}(p)$ for the considered values of L and thus larger $\delta^2(p)$ at points $p = (p^* - \Delta p)$ and $p = (p^* + \Delta p)$ than at $p = p^*$. This means that the true value of p_c is somewhere inside the interval $(p^* - \Delta p, p^* + \Delta p)$.

On the other hand, for $\Delta p = 10^{-6}$ (see Figure 5.3) we cannot easily identify the “intersection point”. The reason for this lies in too weak statistics, i.e., too small number R of the simulation repetition. The precision of determining the value of $P_{\max}(n)$ —i.e. $\bar{X}(n; N)$ in Equation (4)—is $1/R$ and affects the selection of Δp value, which allows observing a clear $\delta^2(p)$ minimum for $p = p^*$, with a simultaneous clear spread of points $L^{\beta/\nu} \cdot P_{\max}(p)$ for various L at $p = p^* - \Delta p$ and $p = p^* + \Delta p$. Hence, we consider $\Delta p = 10^{-5}$ as the uncertainty of the determined p_c . Moreover, plotting $L^{\beta/\nu} \cdot P_{\max}(p)$ for finite L according to Equation (1) allows us to eliminate, at least partially, the effect of finite sizes on the accuracy of determining p_c .

In Figure 4.2 we clearly observe two series of data, roughly for p_c below and above 0.2. The latter correspond to SQ-7, SQ-2,7, SQ-3,7, SQ-5,7, SQ-2,3,7, SQ-2,5,7, SQ-3,5,7 and SQ-2,3,5,7. These neighborhoods are the so-called inflated neighborhoods, which means that they have partners with lower indexed neighborhoods with the same p_c and z . These partners are presented in Figure 6.

Similarly to neighborhoods with smaller ranges, the power-law dependence of the percolation threshold on the effective coordination number with exponent w close to $-1/2$ is observed. The power law is obtained after excluding p_c of the inflated neighborhoods (marked by \times in Figure 4.3) from the fitting procedure.

Introducing the effective coordination number ζ partially eliminates the degeneration (see Figure 4.2) strongly observed in the dependence on $p_c(z)$ (see Fig-

ure 4.1). For $p_c(\zeta)$, we still observe this degeneration in several cases, such as

- $\zeta(\text{SQ-1,3,7}) = \zeta(\text{SQ-6,7})$,
- $\zeta(\text{SQ-1,2,3,7}) = \zeta(\text{SQ-2,6,7})$,
- $\zeta(\text{SQ-1,3,5,7}) = \zeta(\text{SQ-5,6,7})$,
- $\zeta(\text{SQ-1,3,4,7}) = \zeta(\text{SQ-4,6,7})$,
- $\zeta(\text{SQ-1,2,3,4,7}) = \zeta(\text{SQ-2,4,6,7})$,
- $\zeta(\text{SQ-1,3,4,5,7}) = \zeta(\text{SQ-4,5,6,7})$,
- $\zeta(\text{SQ-1,2,3,4,5,7}) = \zeta(\text{SQ-2,4,5,6,7})$.

This degeneration in distinguishing neighborhoods based only on the scalar variable can be resolved after normalization of ζ to the total number of sites in the neighborhood z . The fraction ζ/z is nothing else but the mean distance

$$\bar{r} = \frac{1}{z} \sum_i z_i r_i \quad (8)$$

of sites in the neighborhood to the central site. We can call it the mean radius of the neighborhood.

In Figure 7 we show the dependence p_c on the mean radius \bar{r} for the 131 neighborhoods that contain sites in the range smaller than or equal to $\bar{r}(\text{SQ-7}) = \sqrt{10}$. In this plot, only three neighborhoods have identical mean radius $\bar{r}(\text{SQ-3}) = \bar{r}(\text{SQ-1,6}) = \bar{r}(\text{SQ-1,3,6}) = 2$ (these three neighborhoods are marked by \times). Furthermore, we can empirically determine the lower limit of the percolation threshold for complex neighborhoods as

$$p_c(\text{SQ}) \geq \frac{p_c(\text{SQ-1})}{\bar{r}^2}. \quad (9)$$

This limit also holds for extended neighborhoods with sites beyond the 7th coordination zone, for example SQ-1,2,3,4,5,6,7,8, SQ-1,2,3,4,5,6,7,8,9 and SQ-1,2,3,4,5,6,7,8,9,10 (p_c values for these neighborhoods are taken after Reference [73]). The results for extended neighborhoods (which are both complex and compact, marked by $+$ in Figure 7) touch the boundary line of inequality (9).

Also in Reference [73]—from which we took values of p_c for SQ-1,2,3,4,5,6,7,8, SQ-1,2,3,4,5,6,7,8,9, SQ-1,2,3,4,5,6,7,8,9,10 neighborhoods—Xun *et al.* studied, among other things, also the percolation thresholds for regular lattices with compact extended-range neighborhoods in two dimensions. For all Archimedean lattices and up to the 10th nearest neighbors, they show the dependence z versus $1/p_c$ (Figure 7 in Reference [73]) and $-1/\ln(1-p_c)$ (Figure 8 in Reference [73]). For new variables $y = z$ and $x = 1/p_c$ or $x = -1/\ln(1-p_c)$ in both cases the slope of the straight line close to the experimental points is $y = 4.521x$ and the value of $4.521 = 4\eta_c$ comes from the critical filling factor of circular neighborhoods in two dimensions (i.e. for continuous percolation

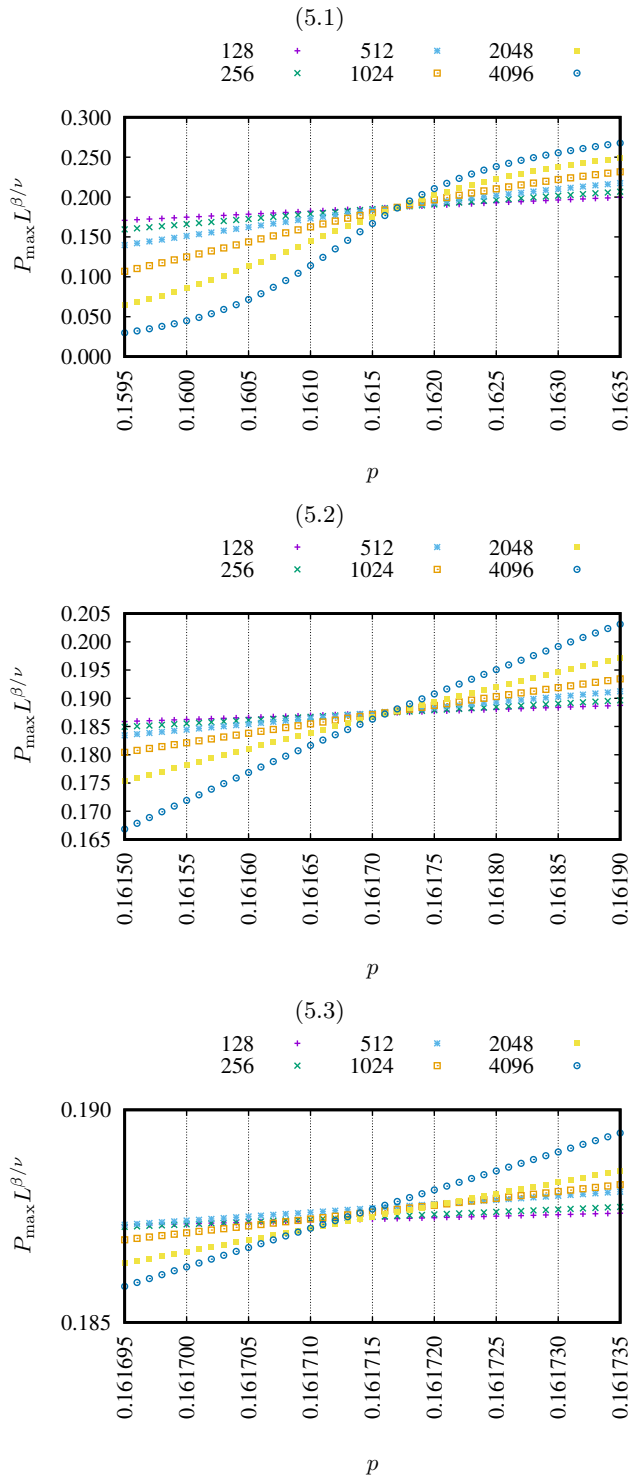


FIG. 5: Dependencies $L^{\beta/\nu} \cdot P_{\max}(p)$ for various values of the separation Δp : (5.1) 10^{-4} , (5.2) 10^{-5} , (5.3) 10^{-6} .

With assumed number of repetition of simulations ($R = 10^5$) value $\Delta p = 10^{-6}$ is insufficient to see clear “single crossing-point” and to identify $p = p^*$

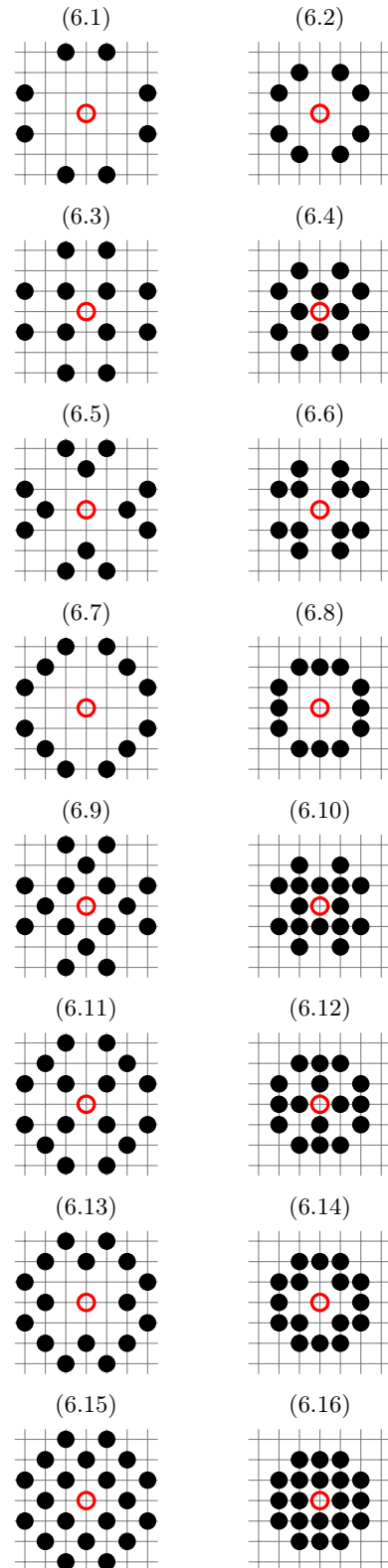


FIG. 6: Inflated neighborhoods (6.1) sq-7, (6.3) sq-2,7, (6.5) sq-3,7, (6.7) sq-5,7, (6.9) sq-2,3,7, (6.11) sq-2,5,7, (6.13) sq-3,5,7, (6.15) sq-2,3,5,7 and their lower indexed partners (6.2) sq-4, (6.4) sq-1,4, (6.6) sq-2,4, (6.8) sq-3,4, (6.10) sq-1,2,4, (6.12) sq-1,3,4, (6.14) sq-2,3,4, (6.16) sq-1,2,3,4

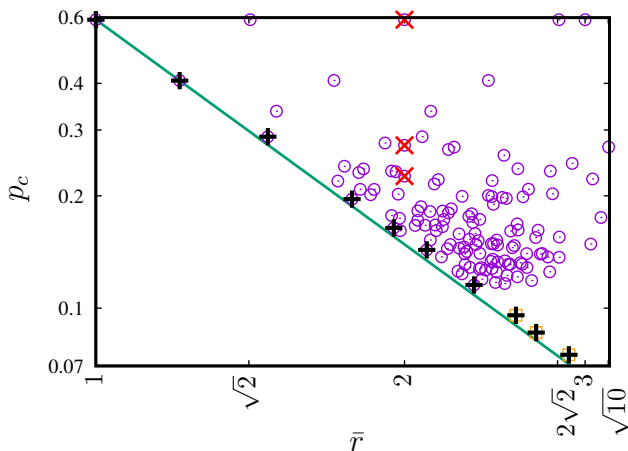


FIG. 7: Dependence of percolation threshold p_c on mean radius \bar{r} of the neighborhoods. The mean radius \bar{r} uniquely identifies neighborhoods except of three neighborhoods SQ-3, SQ-1,6 and SQ-1,3,6 all with mean radius equal to two. These three neighborhoods are marked by crosses (\times). The open squares (\square) correspond to SQ-1,2,3,4,5,6,7,8, SQ-1,2,3,4,5,6,7,8,9, SQ-1,2,3,4,5,6,7,8,9,10 neighborhoods (after Reference [73]). Pluses (+) show p_c associated with compact neighborhoods

of discs, where $\eta_c = 1.12808737(6)$ [89]). The experimental data for z vs. $1/p_c$ lie below this straight line as compact neighborhoods become solid discs in the limit of $z \rightarrow \infty$. In Figure 8 the reciprocal of p_c both from our work (against r^2) and the continuous percolation limit (from Reference [73], against z) are presented. As we can see, for compact neighborhoods (at least for the square lattice and site percolation problem), we can confine percolation thresholds p_c between two curves.

To conclude, we calculated 64 percolation thresholds for neighborhoods containing sites from the 7th coordination zone, of which 63 are evaluated for the first time. The obtained values of p_c follow the early prediction of $p_c(\zeta)$, which is given by the power law $p_c \propto \zeta^{-w}$ with the exponent w close to $1/2$. Investigating the degeneration of p_c versus ζ allowed us to determine the lower limit p_c as dependent on the inverse square of the mean distance \bar{r} of sites in the neighborhoods. The latter touches the boundary line for the extended (compact) neighborhoods. These results enrich earlier studies of site percolation for compact neighborhoods [73] where p_c values were restricted by the limitation predicted by $1/p_c > z/(4\eta_c)$, where η_c is the critical filling factor for the continuous percolation of discs. Finally, we also recalculated $p_c(\text{SQ-2,4}) = 0.23288$, which means that its value provided in Reference [77] as $p_c(\text{SQ-2,4}) = 0.225$ was clearly underestimated.

Further studies may concentrate on the estimation of the percolation thresholds p_c for triangular or honeycomb lattices with complex neighborhoods containing sites from the 7th coordination zone or validation of

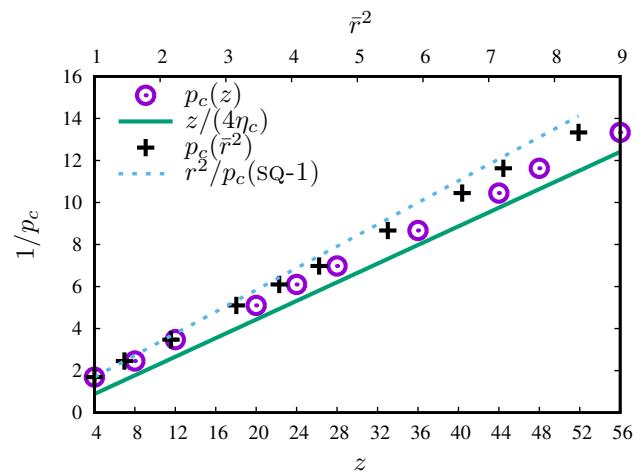


FIG. 8: Dependence of reciprocal percolation threshold $1/p_c$ on \bar{r}^2 and z of the neighborhoods. Data for SQ-1,2,3,4,5,6,7,8, SQ-1,2,3,4,5,6,7,8,9, SQ-1,2,3,4,5,6,7,8,9,10 neighborhoods are taken from Reference [73] together with the continuous percolation limit of the discs ($4\eta_c$)

Equation (9) for other lattices.

ACKNOWLEDGMENTS

Authors gratefully acknowledge Poland's high-performance computing infrastructure PLGrid (HPC Centers: ACK Cyfronet AGH) for providing computer facilities and support within computational grant no. PLG/2023/016295.

Appendix A:

In Listing 1 the `boundaries()` procedure to be replaced in the original program published in Reference [86] is presented. The example corresponds to the SQ-7 neighborhood.

Listing 1: `boundaries()` procedure for SQ-7 neighborhood to be inserted in Newman–Ziff algorithm code published in Reference [86]

```

1 // SQ-7
2 #define L 9          /* Linear dimension */
3 #define Z 8
4 #define N (L*L)
5
6 int nn[N][Z];      /* Nearest neighbors */
7
8 void boundaries() {
9     int i,j;
10    for(i=0; i<N; i++) {
11        // 7nn core:
12        nn[i][0] = (N+i +L+3)%N;
13        nn[i][1] = (N+i +L-3)%N;
14        nn[i][2] = (N+i -L+3)%N;
15        nn[i][3] = (N+i -L-3)%N;

```

```

16 nn[i][4] = (N+i +3*L+1)%N;
17 nn[i][5] = (N+i +3*L-1)%N;
18 nn[i][6] = (N+i -3*L+1)%N;
19 nn[i][7] = (N+i -3*L-1)%N;
20 // 7nn left border:
21 if(i%L==0) {
22     nn[i][1] = (N+L+i +L-3)%N;
23     nn[i][3] = (N+L+i -L-3)%N;
24     nn[i][5] = (N+L+i +3*L-1)%N;
25     nn[i][7] = (N+L+i -3*L-1)%N; }
26 if(i%L==1 || i%L==2) {
27     nn[i][1] = (N+L+i +L-3)%N;
28     nn[i][3] = (N+L+i -L-3)%N; }
29 // 7nn right border:
30 if((i+3)%L==0 || (i+2)%L==0) {
31     nn[i][0] = (N-L+i +L+3)%N;
32     nn[i][2] = (N-L+i -L+3)%N; }
33 if((i+1)%L==0) {
34     nn[i][0] = (N-L+i +L+3)%N;
35     nn[i][2] = (N-L+i -L+3)%N;
36     nn[i][4] = (N-L+i +3*L+1)%N;
37     nn[i][6] = (N-L+i -3*L+1)%N; }
38 }
39 }

```

- [1] D. Stauffer and A. Aharony, *Introduction to Percolation Theory*, 2nd ed. (Taylor and Francis, London, 1994).
- [2] B. Bollobás and O. Riordan, *Percolation* (Cambridge UP, Cambridge, 2006).
- [3] M. Sahimi, *Applications of Percolation Theory* (Taylor and Francis, London, 1994).
- [4] H. Kesten, *Percolation Theory for Mathematicians* (Birkhauser, Boston, 1982).
- [5] A. A. Saberi, Recent advances in percolation theory and its applications, *Physics Reports* **578**, 1 (2015).
- [6] M. Li, R.-R. Liu, L. Lü, M.-B. Hu, S. Xu, and Y.-C. Zhang, Percolation on complex networks: Theory and application, *Physics Reports* **907**, 1 (2021).
- [7] M. F. Sykes and J. W. Essam, Exact critical percolation probabilities for site and bond problems in two dimensions, *Journal of Mathematical Physics* **5**, 1117 (1964).
- [8] R. M. Ziff and C. R. Scullard, Exact bond percolation thresholds in two dimensions, *Journal of Physics A: Mathematical and General* **39**, 15083 (2006).
- [9] C. R. Scullard, Exact site percolation thresholds using a site-to-bond transformation and the star-triangle transformation, *Physical Review E* **73**, 016107 (2006).
- [10] J. L. Jacobsen, High-precision percolation thresholds and Potts-model critical manifolds from graph polynomials, *Journal of Physics A: Mathematical and Theoretical* **47**, 135001 (2014).
- [11] F. Coupette and T. Schilling, Exactly solvable percolation problems, *Physical Review E* **105**, 044108 (2022).
- [12] R. K. Akhunzhanov, A. V. Eserkepov, and Y. Y. Tarasevich, Exact percolation probabilities for a square lattice: Site percolation on a plane, cylinder, and torus, *Journal of Physics A: Mathematical and Theoretical* **55**, 204004 (2022).
- [13] S. R. Broadbent and J. M. Hammersley, Percolation processes: I. Crystals and mazes, *Mathematical Proceedings of the Cambridge Philosophical Society* **53**, 629 (1957).
- [14] J. M. Hammersley, Percolation processes: II. The connective constant, *Mathematical Proceedings of the Cambridge Philosophical Society* **53**, 642 (1957).
- [15] D. Soto-Gomez, L. Vazquez Juiz, P. Perez-Rodriguez, J. Eugenio Lopez-Periago, M. Paradelo, and J. Koestel, Percolation theory applied to soil tomography, *Geoderma* **357**, 113959 (2020).
- [16] S. F. Bolandtaba and A. Skauge, Network modeling of eor processes: A combined invasion percolation and dynamic model for mobilization of trapped oil, *Transport in Porous Media* **89**, 357 (2011).
- [17] S. C. Mun, M. Kim, K. Prakashan, H. J. Jung, Y. Son, and O. O. Park, A new approach to determine rheological percolation of carbon nanotubes in microstructured polymer matrices, *Carbon* **67**, 64 (2014).
- [18] B. Ghanbarian, F. Liang, and H.-H. Liu, Modeling gas relative permeability in shales and tight porous rocks, *Fuel* **272**, 117686 (2020).
- [19] B. G. Ueland, N. H. Jo, A. Sapkota, W. Tian, M. Masters, H. Hodovanets, S. S. Downing, C. Schmidt, R. J. McQueeney, S. L. Bud'ko, A. Kreyssig, P. C. Canfield, and A. I. Goldman, Reduction of the ordered magnetic moment and its relationship to Kondo coherence in $Ce_{1-x}La_xCu_2Ge_2$, *Physical Review B* **97**, 165121 (2018).
- [20] L. Keeney, C. Downing, M. Schmidt, M. E. Pemble, V. Nicolosi, and R. W. Whatmore, Direct atomic scale determination of magnetic ion partition in a room temperature multiferroic material, *Scientific Reports* **7**, 1737 (2017).
- [21] P. Buczek, L. M. Sandratskii, N. Buczek, S. Thomas, G. Vignale, and A. Ernst, Magnons in disordered nonstoichiometric low-dimensional magnets, *Physical Review B* **94**, 054407 (2016).
- [22] Y. Yiu, P. Bonfá, S. Sanna, R. De Renzi, P. Carretta, M. A. McGuire, A. Huq, and S. E. Nagler, Tuning the magnetic and structural phase transitions of $PrFeAsO$ via Fe/Ru spin dilution, *Physical Review B* **90**, 064515 (2014).
- [23] M. Grady, Possible new phase transition in the 3D Ising model associated with boundary percolation, *Journal of Physics: Condensed Matter* **35**, 285401 (2023).
- [24] J. Jeong, K. J. Park, E.-J. Cho, H.-J. Noh, S. B. Kim, and H.-D. Kim, Electronic structure change of $NiS_{2-x}Se_x$ in the metal-insulator transition probed by X-ray absorption spectroscopy, *Journal of the Korean Physical Society* **72**, 111 (2018).
- [25] A. Avella, A. M. Oles, and P. Horsch, Defect-induced orbital polarization and collapse of orbital order in doped vanadium perovskites, *Physical Review Letters* **122**, 127206 (2019).
- [26] L. Cheng, P. Yan, X. Yang, H. Zou, H. Yang, and H. Liang, High conductivity, percolation behavior and dielectric relaxation of hybrid ZIF-8/CNT composites, *Journal of Alloys and Compounds* **825**, 154132 (2020).
- [27] F. Xu, Z. Xu, and B. I. Yakobson, Site-percolation threshold of carbon nanotube fibers—Fast inspection of percolation with Markov stochastic theory, *Physica A* **407**, 341 (2014).
- [28] M. Sykes and M. Glen, Percolation processes in 2 dimensions. 1. Low-density series expansions, *Journal of*

- Physics A: Mathematical & General **9**, 87 (1976).
- [29] M. Sykes, D. Gaunt, and M. Glen, Percolation processes in 2 dimensions. 2. Critical concentrations and mean size index, *Journal of Physics A: Mathematical & General* **9**, 97 (1976).
- [30] M. Sykes, D. Gaunt, and M. Glen, Percolation processes in 2 dimensions. 3. High-density series expansions, *Journal of Physics A: Mathematical & General* **9**, 715 (1976).
- [31] M. Sykes, D. Gaunt, and M. Glen, Percolation processes in 2 dimensions. 4. Percolation probability, *Journal of Physics A: Mathematical & General* **9**, 725 (1976).
- [32] D. Gaunt and M. Sykes, Percolation processes in 2 dimensions. 5. Exponent δ_p and scaling theory, *Journal of Physics A: Mathematical & General* **9**, 1109 (1976).
- [33] L. A. Meyers, Contact network epidemiology: Bond percolation applied to infectious disease prediction and control, *Bulletin of the American Mathematical Society* **44**, 63 (2007).
- [34] D.-S. Lee and M. Zhu, Epidemic spreading in a social network with facial masks wearing individuals, *IEEE Transactions on Computational Social Systems* **8**, 1393 (2021).
- [35] R. M. Ziff, Percolation and the pandemic, *Physica A* **568**, 125723 (2021).
- [36] K. Malarz, S. Kaczanowska, and K. Kułakowski, Are forest fires predictable?, *International Journal of Modern Physics C* **13**, 1017 (2002).
- [37] N. Guisoni, E. S. Loscar, and E. V. Albano, Phase diagram and critical behavior of a forest-fire model in a gradient of immunity, *Physical Review E* **83**, 011125 (2011).
- [38] A. Simeoni, P. Salinesi, and F. Morandini, Physical modelling of forest fire spreading through heterogeneous fuel beds, *International Journal of Wildland Fire* **20**, 625 (2011).
- [39] G. Camelo-Neto and S. Coutinho, Forest-fire model with resistant trees, *Journal of Statistical Mechanics—Theory and Experiments* **2011**, P06018 (2011).
- [40] S. R. Abades, A. Gaxiola, and P. A. Marquet, Fire, percolation thresholds and the savanna forest transition: A neutral model approach, *Journal of Ecology* **102**, 1386 (2014).
- [41] J. E. Ramírez, C. Pajares, M. I. Martínez, R. Rodríguez Fernández, E. Molina-Gayosso, J. Lozada-Lechuga, and A. Fernández Téllez, Site-bond percolation solution to preventing the propagation of *Phytophthora zoospores* on plantations, *Physical Review E* **101**, 032301 (2020).
- [42] D. Rosales Herrera, J. E. Ramírez, M. I. Martínez, H. Cruz-Suárez, A. Fernández Téllez, J. F. López-Olguín, and A. Aragón García, Percolation-intercropping strategies to prevent dissemination of *phytopathogens* on plantations, *Chaos* **31**, 063105 (2021).
- [43] D. R. Herrera, J. Velázquez-Castro, A. F. Téllez, J. F. López-Olguín, and J. E. Ramírez, Site percolation threshold of composite square lattices and its agroecology applications, *Physical Review E* **109**, 014304 (2024).
- [44] W. Cao, L. Dong, L. Wu, and Y. Liu, Quantifying urban areas with multi-source data based on percolation theory, *Remote Sensing of Environment* **241**, 111730 (2020).
- [45] M. K. M. Ng, Z. Shabrina, S. Sarkar, H. Han, and C. Petit, From urban clusters to megaregions: mapping Australia’s evolving urban regions, *Computational Urban Science* **4**, 28 (2024).
- [46] M. Alguero, M. Perez-Cerdan, R. P. del Real, J. Ricote, and A. Castro, Novel Aurivillius $\text{Bi}_4\text{Ti}_{3-2x}\text{Nb}_x\text{Fe}_x\text{O}_{12}$ phases with increasing magnetic-cation fraction until percolation: A novel approach for room temperature multiferroism, *Journal of Materials Chemistry C* **8**, 12457 (2020).
- [47] A. Moreira, J. Andrade, and D. Stauffer, Sznajd social model on square lattice with correlated percolation, *International Journal of Modern Physics C* **12**, 39 (2001).
- [48] K. Malarz and M. Wołoszyn, Thermal properties of structurally balanced systems on classical random graphs, *Chaos* **33**, 073115 (2023).
- [49] L. Cirigliano, C. Castellano, and G. Timár, Extended-range percolation in complex networks, *Physical Review E* **108**, 044304 (2023).
- [50] S. Bartolucci, F. Caccioli, and P. Vivo, A percolation model for the emergence of the Bitcoin Lightning Network, *Scientific Reports* **10**, 4488 (2020).
- [51] M. Beddoe, T. Gözl, M. Barkey, E. Bau, M. Godejohann, S. A. Maier, F. Keilmann, M. Moldovan, D. Prodan, N. Ilie, and A. Tittl, Probing the micro- and nanoscopic properties of dental materials using infrared spectroscopy: A proof-of-principle study, *Acta Biomaterialia* **168**, 309 (2023).
- [52] P. Grassberger, Critical percolation in high dimensions, *Physical Review E* **67**, 036101 (2003).
- [53] M. F. Sykes and J. W. Essam, Critical percolation probabilities by series methods, *Physical Review* **133**, A310 (1964).
- [54] A. Sur, J. L. Lebowitz, J. Marro, M. H. Kalos, and S. Kirkpatrick, Monte carlo studies of percolation phenomena for a simple cubic lattice, *Journal of Statistical Physics* **15**, 345 (1976).
- [55] D. Gaunt and M. Sykes, Series study of random percolation in 3 dimensions, *Journal of Physics A: Mathematical & General* **16**, 783 (1983).
- [56] C. Lorenz and R. Ziff, Universality of the excess number of clusters and the crossing probability function in three-dimensional percolation, *Journal of Physics A: Mathematical & General* **31**, 8147 (1998).
- [57] Ł. Kurzawski and K. Malarz, Simple cubic random-site percolation thresholds for complex neighbourhoods, *Reports on Mathematical Physics* **70**, 163 (2012).
- [58] M. Kotwica, P. Groniek, and K. Malarz, Efficient space virtualisation for Hoshen–Kopelman algorithm, *International Journal of Modern Physics C* **30**, 1950055 (2019).
- [59] P. Zhao, J. Yan, Z. Xun, D. Hao, and R. M. Ziff, Site and bond percolation on four-dimensional simple hypercubic lattices with extended neighborhoods, *Journal of Statistical Mechanics: Theory and Experiment* **2022**, 033202 (2022).
- [60] G. Paul, R. M. Ziff, and H. E. Stanley, Percolation threshold, Fisher exponent, and shortest path exponent for four and five dimensions, *Physical Review E* **64**, 026115 (2001).
- [61] Z. Xun, D. Hao, and R. M. Ziff, Extended-range percolation in five dimensions (2023), [arXiv:2308.15719 \[cond-mat.stat-mech\]](https://arxiv.org/abs/2308.15719).
- [62] S. Van der Marck, Calculation of percolation thresholds in high dimensions for FCC, BCC and diamond lattices, *International Journal of Modern Physics C* **9**, 529 (1998).
- [63] Z. Koza and J. Pola, From discrete to continuous percolation in dimensions 3 to 7, *Journal of Statistical Mechanics: Theory and Experiment* **2016**, 103206 (2016).
- [64] A. Haji-Akbari and R. M. Ziff, Percolation in networks with voids and bottlenecks, *Physical Review E* **79**,

- 021118 (2009).
- [65] S. Mitra, D. Saha, and A. Sensharma, Percolation in a distorted square lattice, *Physical Review E* **99**, 012117 (2019).
- [66] S. Mitra, D. Saha, and A. Sensharma, Percolation in a simple cubic lattice with distortion, *Physical Review E* **106**, 034109 (2022).
- [67] S. Mitra and A. Sensharma, Site percolation in distorted square and simple cubic lattices with flexible number of neighbors, *Physical Review E* **107**, 064127 (2023).
- [68] M.-A. M. Cruz, J. P. Ortiz, M. P. Ortiz, and A. Balankin, Percolation on fractal networks: A survey, *Fractal and Fractional* **7**, 231 (2023).
- [69] N. W. Dalton, C. Domb, and M. F. Sykes, Dependence of critical concentration of a dilute ferromagnet on the range of interaction, *Proceedings of the Physical Society* **83**, 496 (1964).
- [70] C. Domb and N. W. Dalton, Crystal statistics with long-range forces: I. The equivalent neighbour model, *Proceedings of the Physical Society* **89**, 859 (1966).
- [71] K. Malarz, Universality of percolation thresholds for two-dimensional complex non-compact neighborhoods, *Physical Review E* **109**, 034108 (2024).
- [72] Z. Xun, D. Hao, and R. M. Ziff, Site percolation on square and simple cubic lattices with extended neighborhoods and their continuum limit, *Physical Review E* **103**, 022126 (2021).
- [73] Z. Xun, D. Hao, and R. M. Ziff, Site and bond percolation thresholds on regular lattices with compact extended-range neighborhoods in two and three dimensions, *Physical Review E* **105**, 024105 (2022).
- [74] Z. Xun and D. Hao, Monte Carlo simulation of bond percolation on square lattice with complex neighborhoods, *Acta Physica Sinica* **71**, 066401 (2022), in Chinese.
- [75] K. Malarz and S. Galam, Square-lattice site percolation at increasing ranges of neighbor bonds, *Physical Review E* **71**, 016125 (2005).
- [76] S. Galam and K. Malarz, Restoring site percolation on damaged square lattices, *Physical Review E* **72**, 027103 (2005).
- [77] M. Majewski and K. Malarz, Square lattice site percolation thresholds for complex neighbourhoods, *Acta Physica Polonica B* **38**, 2191 (2007).
- [78] K. Malarz, Simple cubic random-site percolation thresholds for neighborhoods containing fourth-nearest neighbors, *Physical Review E* **91**, 043301 (2015).
- [79] K. Malarz, Site percolation thresholds on triangular lattice with complex neighborhoods, *Chaos* **30**, 123123 (2020).
- [80] K. Malarz, Percolation thresholds on triangular lattice for neighbourhoods containing sites up to the fifth coordination zone, *Physical Review E* **103**, 052107 (2021).
- [81] K. Malarz, Random site percolation on honeycomb lattices with complex neighborhoods, *Chaos* **32**, 083123 (2022).
- [82] K. Malarz, Random site percolation thresholds on square lattice for complex neighborhoods containing sites up to the sixth coordination zone, *Physica A* **632**, 129347 (2023).
- [83] Z. Xun, D. Hao, and R. M. Ziff, Site percolation on square and simple cubic lattices with extended neighborhoods and their continuum limit, *Physical Review E* **103**, 022126 (2021).
- [84] V. Privman, Finite-size scaling theory, in *Finite size scaling and numerical simulation of statistical systems*, edited by V. Privman (World Scientific, Singapore, 1990) pp. 1–98.
- [85] D. P. Landau and K. Binder, *A Guide to Monte Carlo Simulations in Statistical Physics*, 3rd ed. (Cambridge University Press, Cambridge, 2009).
- [86] M. E. J. Newman and R. M. Ziff, Fast Monte Carlo algorithm for site or bond percolation, *Physical Review E* **64**, 016706 (2001).
- [87] See Supplemental Material at <https://doi.org/10.58032/AGH/SWJZKD> for dependencies $P_{\max} L^{\beta/\nu}(p)$ for all neighborhoods containing sites from the 7th coordination zone.
- [88] N. Bastas, K. Kosmidis, P. Giazitzidis, and M. Maragakis, Method for estimating critical exponents in percolation processes with low sampling, *Physical Review E* **90**, 062101 (2014).
- [89] S. Mertens and C. Moore, Continuum percolation thresholds in two dimensions, *Physical Review E* **86**, 061109 (2012).